Phytochemical Profiling of *Gynura procumbens* (Lour.) Merr. Leaves and Stem Extracts Using UHPLC-Q-Orbitrap HRMS

Dewi Anggraini Septaningsih[1,2], Cecep Abdurohman Putra[1], Irma Herawati Suparto[1,3,4], Suminar Setiati Achmadi[1,3], Rudi Heryanto[1,2,3], and Mohamad Rafi[1,2,3*]

[1]*Department of Chemistry, Faculty of Mathematics and Natural Sciences, IPB University, Jl. Tanjung Kampus IPB Dramaga, Bogor 16680, Indonesia*

[2]*Advanced Research Laboratory, Institute of Research and Community Services, IPB University, Jl. Palem Kampus IPB Dramaga, Bogor 16680, Indonesia*

[3]*Tropical Biopharmaca Research Center-Institute of Research and Community Services, IPB University, Jl. Taman Kencana No. 3, Kampus IPB Taman Kencana, Bogor 16128, Indonesia*

[4]*Primate Research Center, Institute of Research and Community Services, IPB University, Jl. Lodaya II No. 5 Kampus IPB Lodaya, Bogor 16151, Indonesia*

* ***Corresponding author:***

tel: +62-251-8624567
email: mra@apps.ipb.ac.id

Received: April 20, 2022
Accepted: June 29, 2022

DOI: 10.22146/ijc.74236

Abstract: *In Indonesia,* Gynura procumbens *(Lour.) Merr., known as Longevity Spinach or* Sambung Nyawa*, is commonly grown in tropical and subtropical Asian countries. Many biological activities of* G. procumbens *have been reported. As we know, the composition and concentration of metabolites, as well as plant parts will significantly affect the biological activities. In this work, UHPLC-Q-Orbitrap-HRMS was used for the putative identification of metabolites present in 70% ethanol extract of* G. procumbens *leaves and stem extract. Also, we performed clustering of* G. procumbens *leaves and stem extracts using principal component analysis (PCA) with the peak area of the identified metabolites as the variable. Thirty-one metabolites were identified, and the number of identified peaks in the leaves is higher than in the stem. Those identified metabolites are phenolics, fatty acids, oxo monocarboxylic acids, porphyrins, and chlorophyll fragments. The PCA results showed that the leaves and stem extracts could be grouped, indicating that the composition and concentration of detected compounds differed.*

Keywords: Gynura procumbens*; metabolomics; phytochemical profiling; UHPLC-Q-Orbitrap-HRMS*

■ INTRODUCTION

Gynura procumbens (Lour.) Merr. (Longevity Spinach or Sambung Nyawa) belongs to the Asteraceae family. This medicinal plant grows in tropical and subtropical Asian countries such as Indonesia, Malaysia, China, and Vietnam. Several biological activities of this species have been acknowledged, such as antimicrobial, antioxidant, anti-inflammatory, anticancer, antihypertensive, and antihyperglycemic [1-3]. The biological activity is affected by the presence of its metabolites. The detected bioactive metabolites in the leaves of *G. procumbens* include phenolic acids, flavonoids, saponins, tannins, terpenoids, and steroid glycosides [4-6].

The composition and concentration of metabolites strongly affect the consistency of the biological activity of medicinal plants. It is widely known that the composition and the concentration of bioactive metabolites depend on several factors, i.e., the growth site, the age of harvest, the part of the plant, the post-harvest treatment, and the processing of commercial products [7-10]. To determine the overall metabolite profile detected due to those various factors and experimental treatments, we can use the untargeted

metabolomics approach, i.e., metabolite profiling or fingerprinting using ultrahigh-performance liquid chromatography-quadrupole-orbitrap-high-resolution mass spectrometer (UHPLC-Q-Orbitrap-HRMS). This analytical instrument has several advantages, such as high sensitivity and selectivity and the ability to separate and identify valuable metabolites [11].

The leaves and the stem of *G. procumbens* have been reported to differ in their biological activities [1]. The phenolic profile of the *G. procumbens* leaves has been previously reported [12]. However, the leaves and stem metabolites are not solely known through phytochemical qualitative analysis yet. In addition, there are no reported papers on the distribution of chemical compounds in the leaves and stems. Therefore, by using UHPLC-Q-Orbitrap-HRMS, we aim to putatively identify the metabolites and whether the composition and concentration are different in the *G. procumbens* leaves and stem extracts.

■ EXPERIMENTAL SECTION

Materials

G. procumbens leaves and stems were collected from the Tropical Biopharmaca Research Center (TropBRC) medicinal plant garden, IPB University, Bogor, Indonesia. Mr. Taufik Ridwan identified the samples from TropBRC, IPB University. The voucher specimen (BMK 0310122016) was stored in TropBRC, IPB University. Ethanol (LC grade), acetonitrile, and water (LC-MS grade) were purchased from Merck (Darmstadt, Germany). We also used filter paper PTFE 0.22 µm from Ambala Cantt (India).

Instrumentation

Extractions of *G. procumbens* leaves and stem were performed through ultrasonication (OVAN, Barcelona, Spain) for 30 min. The separation and identification of the metabolites were performed using Vanquish Flex UHPLC in tandem with UHPLC-Q-Orbitrap HRMS equipped with ThermoXCalibur and Compound Discoverer version 2.2 (Thermo Fisher, Waltham, MA, USA).

Procedure

The fresh leaves and stems of G. *procumbens* were dried separately in an oven at 40 °C. The dry sample was then pulverized to a size of 80 mesh. The samples of leaves and stems were separately extracted using 70% ethanol with a ratio of sample and solvent used was 1:10. The sample was sonicated for 30 min. The filtrate was filtered using 0.22 µm PTFE and injected into UHPLC-Q-Orbitrap HRMS afterward. The metabolites were separated using an Accucore C18 column (100 × 2.1 mm, 1.5 µm). The mobile phase was 0.1% formic acid in water (A) and 0.1% formic acid in acetonitrile (B). The flow rate was maintained at 0.2 mL/min, and the injection volume was 5.0 µL. The gradient elution method applied for the separation was as follow: 0.0–12.0 min 10–30% B; 12.0–16.5 min 30–100% B; 16.5–22.0 min 100% B, and conditioning in 22.0–25.0 min with 5% B.

The source of MS ionization was conditioned by ESI positive and negative with Q-Orbitrap mass analyzer. The range of m/z used was 100–1500 *m/z*, automatic gain control (AGC) was set at 3×10^6, and the injection time was set to 100 ms. The collision energy used for fragmentation was 18, 35, and 53 eV. Other conditions were as follows: spray voltage 3.8 kV, the capillary temperature was about 320 °C, and sheath gas and auxiliary gas flow rate were 15 and 3 mL/min, respectively. The scan type used was full MS/dd MS^2, and full scan data in positive and negative were acquired at a resolving power of 70000 FWHM.

The putative identification of metabolites present in the extracts was analyzed using the Compounds Discoverer 2.2 program with several stages: selecting spectra, aligning retention time, detecting unknown compounds, grouping the unknown compounds, predicting compositions, searching the mass list, filling gaps, normalizing areas, and marking background compounds. The mass list employed is an in-house database collected from various scientific journals related to *G. procumbens*.

Clustering of leaves and stem extracts using principal component analysis

Principle component analysis (PCA) was used for clustering the leaves and stem extracts using The Unscrambler X version 10.1 software (CAMO, Oslo, Norway). We used the peak area of 31 metabolites identified in the extract as a variable.

■ RESULTS AND DISCUSSION

The untargeted metabolomics was performed to determine all detectable metabolites present by employing the UHPLC-Q-Orbitrap-HRMS since it gives a shorter analysis time, higher peak intensity, and increased peak resolution [13]. Orbitrap is a mass analyzer that detects analytes to the nearest 0.001 atomic mass unit with a greater mass resolving power [14]. These instruments can be combined with a quadrupole to allow fragmentation and increase the selectivity of method [15]. A chromatogram is a graphical depiction of a sample separating that may be used to identify chemicals and their relative amounts in a mixture. The chromatogram profiles of the leaves and stems extracted in 70% ethanol of *G. procumbens* display slightly different patterns, meaning that the composition and the metabolites' concentration are not similar and will affect the biological activity (Fig. 1). This particular solvent mixture is widely used as a solvent for extraction of various chemicals or nature devoted to pharmaceuticals.

The putative metabolites were identified through an in-house database using the Compound Discoverer 2.2 software. We identified the metabolites putatively by observing the MS2 fragmentation pattern compared to the available literature. Thirty-one compounds are putatively identified in the leaves and stem extracts, such as phenolic acids, flavonoids, hydroxycinnamic acids, fatty acids, oxo monocarboxylic acids, porphyrins, and some products of chlorophyll breakdown (Table 1 and Fig. 2). However, some peaks which arere high intensity have not been successfully identified by using an in-house database.

Phenolic Acids

A total of 8 compounds as phenolic acid groups are identified in the extracts (Table 1). The general fragmentation pattern of phenolic acid is the loss of CO_2, such as in *m/z* 119 for *p*-coumaric acid, m/z 135 for caffeic acid, and *m/z* 179 for sinapic acid [16]. These three compounds have similar biological activities, i.e., antioxidants, anti-inflammatory, and anticancer [17-19]. Another compound that is successfully detected is esculetin (MW 178). The negative mode of the MS spectrum of esculetin (Rt 3.97 min) shows the most abundant fragmentation of esculetin ion is *m/z* 177,

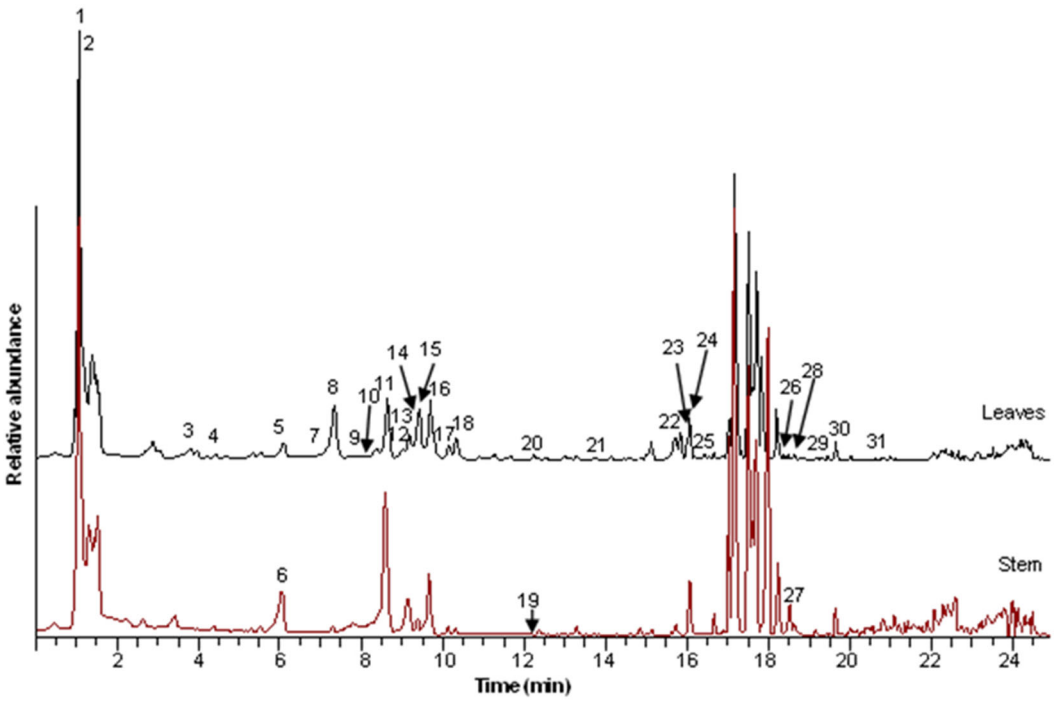

Fig 1. Base peak chromatogram in ionization negative mode of metabolites in *G. procumbens* leaves and stem extracts

No	Compound	Structure
1	Citric acid	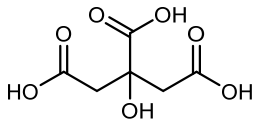
2	Chlorogenic acid	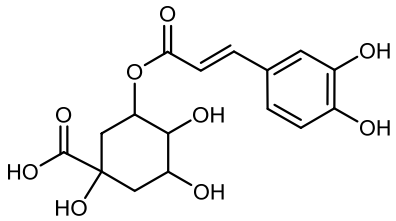
3	Esculetin (Dihydroxycoumarin)	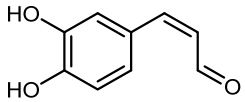
4	Coumaroylquinic acid	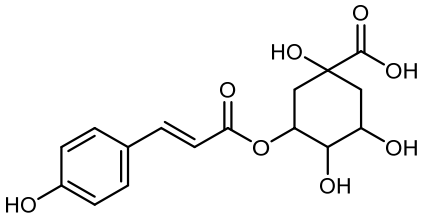
5	*p*-Coumaric acid	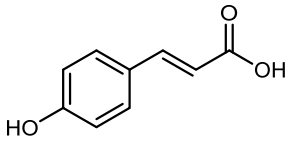
6	1-(3-Indolyl)-2,3-dihydroxy-propan-1-one	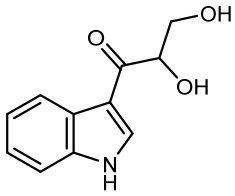
7	Caffeic acid	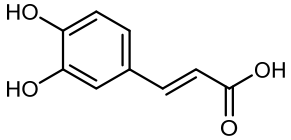
8	Sinapic acid	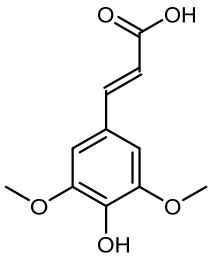
9	4-(2-Hydroxypropoxy)-3,5-dimethyl-phenol	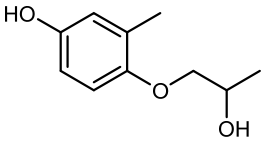

No	Compound	Structure
10	Quercetin 3-*O*-glucopyranoside	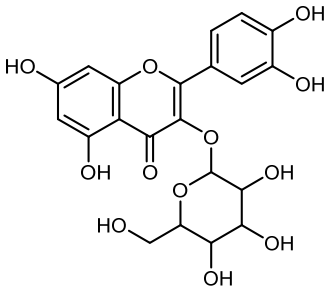
11	Luteolin 7-rutinoside	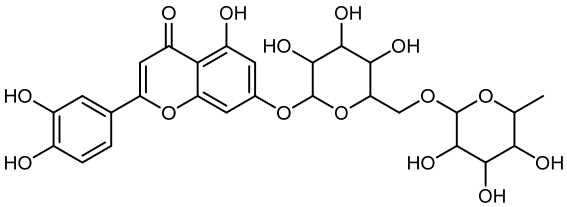
12	Hesperetin	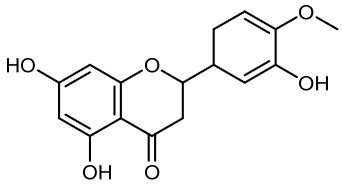
13	Astragalin	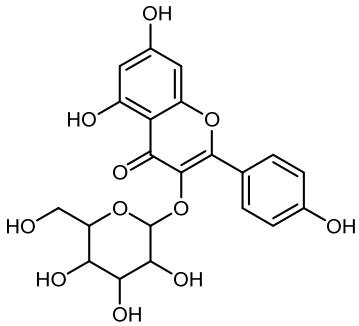
14	Kaempferol-3-*O*-rutinoside	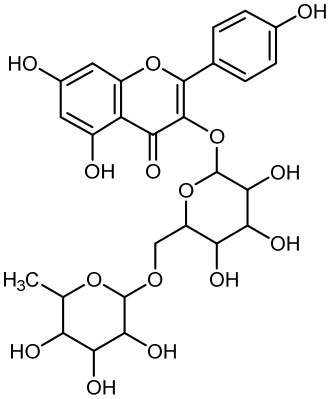
15	3,4-Dicaffeoylquinic acid	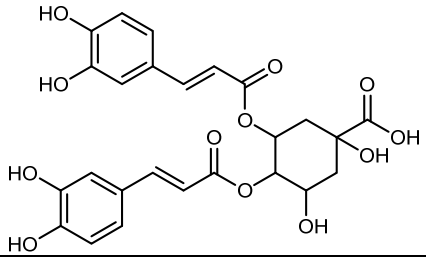

No	Compound	Structure
16	Kaempferol-3-*O*-galactoside	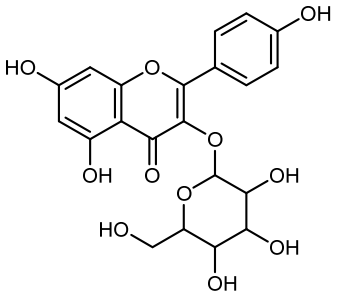
17	Baicalin	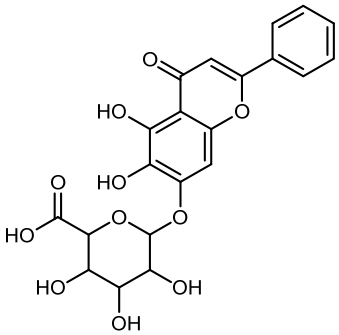
18	3,5-Dicaffeoylquinic acid	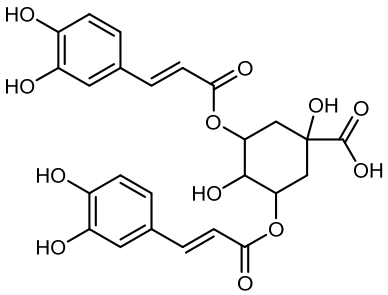
19	Decenedioic acid	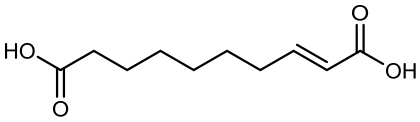
20	4,5-Dicaffeoylquinic acid	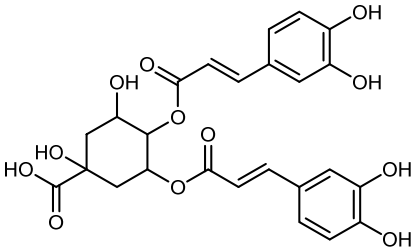
21	Quercetin	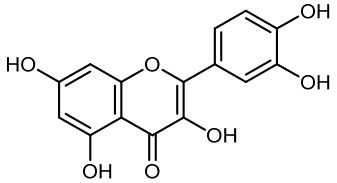
22	Kaempferol	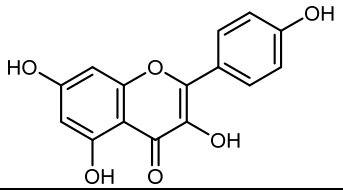

No	Compound	Structure
23	(-)-12-Hydroxy-9,10-dihydrojasmonic acid	
24	5,8,12-Trihydroxy-9-octadecenoic acid	
25	11-Hydroperoxy-12,13-epoxy-9-octadecenoic acid	
26	(9*Z*,12*Z*,15*E*)-Octadecatrienoic acid	
27	(6*E*,9*E*)-Octadecadienoic acid	
28	Ethyl caffeate	
29	Alpha-9(10)-EpODE	
30	Harderoporphyrin	
31	Pheophorbide A	Pheophorbide A

Fig 2. Structure of putative metabolites identified in *G. procumbens*

Table 1. Putative metabolites identified in the *G. procumbens* leaves and stem extracts

No	Compound	Formula	RT (min)	Monoisotopic mass		Error (ppm)	MS^2	Stem	Leaves
				Experimental	Theory				
1	Citric acid	$C_6H_8O_7$	1.26	192.0261	192.0270	-4.58	85, 87, 111, 191	√	√
2	Chlorogenic acid	$C_{16}H_{18}O_9$	1.26	354.0948	354.0951	-0.90	135, 161, 179, 191, 192	-	√
3	Esculetin (Dihydroxycoumarin)	$C_9H_6O_4$	3.97	178.0257	178.0266	-4.89	105, 121, 133, 149, 176, 177	√	√
4	Coumaroylquinic acid	$C_{16}H_{18}O_8$	4.58	338.0998	338.1002	-1.04	93, 111, 163, 173, 191, 337	√	√
5	*p*-Coumaric acid	$C_9H_8O_3$	6.16	164.0464	164.0473	-5.61	163, 119	√	√
6	1-(3-Indolyl)-2,3-dihydroxy-propan-1-one	$C_{11}H_{11}NO_3$	6.23	205.0735	205.0739	-1.71	206	√	-
7	Caffeic acid	$C_9H_8O_4$	6.51	180.0414	180.0423	-4.67	59, 73, 89, 93, 108, 134, 135, 136, 179, 180	-	√
8	Sinapic acid	$C_{11}H_{12}O_5$	7.49	224.0678	224.0685	-2.95	163, 164, 165, 179, 209, 223	√	√
9	4-(2-Hydroxypropoxy)-3,5-dimethyl-Phenol	$C_{11}H_{16}O_3$	8.00	196.1093	196.1099	-3.37	197	√	√
10	Quercetin 3-*O*-glucopyranoside	$C_{21}H_{20}O_{12}$	8.27	464.0950	464.0955	-1.08	165, 229, 257, 303, 304	-	√
11	Luteolin 7-rutinoside	$C_{27}H_{30}O_{15}$	8.58	594.1574	594.1585	-1.77	285	-	√
12	Hesperetin	$C_{16}H_{14}O_6$	8.78	302.0796	302.0790	1.79	118, 136, 301, 302, 303	√	√
13	Astragalin	$C_{21}H_{20}O_{11}$	9.11	448.0996	448.1006	-2.05	227, 255, 285	-	√
14	Kaempferol-3-*O*-rutinoside	$C_{27}H_{30}O_{15}$	9.18	594.1573	594.1585	-1.90	595, 449, 287	-	√
15	3,4-Dicaffeoylquinic acid	$C_{25}H_{24}O_{12}$	9.26	516.1257	516.1268	-2.03	515, 353	√	√
16	Kaempferol-3-*O*-galactoside	$C_{21}H_{20}O_{11}$	9.67	448.0996	448.1006	-2.10	449, 287	-	√
17	Baicalin	$C_{21}H_{18}O_{11}$	10.14	446.0839	446.0849	-2.38	271, 272	-	√
18	3,5-Dicaffeoylquinic acid	$C_{25}H_{24}O_{12}$	10.50	516.1259	516.1268	-1.72	515, 353	√	√
19	Decenedioic acid	$C_{10}H_{16}O_4$	12.06	200.1042	200.1049	-3.35	67, 87, 111, 137, 151, 155, 181, 199	√	-
20	4,5-Dicaffeoylquinic acid	$C_{25}H_{24}O_{12}$	12.42	516.1262	516.1268	-1.10	515, 353	√	√
21	Quercetin	$C_{15}H_{10}O_7$	13.92	302.0424	302.0427	-0.83	121, 151, 178, 273, 301	-	√
22	Kaempferol	$C_{15}H_{10}O_6$	16.01	286.0471	286.0477	-2.34	107, 145, 185, 285, 287	-	√
23	(-)-12-Hydroxy-9,10-dihydrojasmonic acid	$C_{12}H_{20}O_4$	16.21	228.1356	228.1362	-2.37	227	√	√
24	5,8,12-Trihydroxy-9-octadecenoic acid	$C_{18}H_{34}O_5$	16.25	330.2404	330.2406	-0.82	329	√	√
25	11-Hydroperoxy-12,13-epoxy-9-octadecenoic acid	$C_{18}H_{32}O_5$	16.40	328.2247	328.2250	-0.82	111, 197, 291, 327	-	√
26	(9*Z*,12*Z*,15*E*)-Octadecatrienoic acid	$C_{18}H_{30}O_2$	18.40	278.2233	278.2246	-4.78	173, 177, 195, 209, 261, 279	-	√
27	(6*E*,9*E*)-Octadecadienoic acid	$C_{18}H_{32}O_2$	18.63	280.2394	280.2402	-3.07	281	√	-
28	Ethyl caffeate	$C_{11}H_{12}O_4$	18.77	208.0729	208.0736	-3.03	133, 207, 208, 209	√	√
29	alpha-9(10)-EpODE	$C_{18}H_{30}O_3$	18.85	294.2187	294.2195	-2.79	293	-	√
30	Harderoporphyrin	$C_{35}H_{36}N_4O_6$	19.44	608.2600	608.2635	-5.74	609	√	√
31	Pheophorbide A	$C_{35}H_{36}N_4O_5$	20.51	592.2655	592.2686	-5.13	593, 565, 533, 505, 460	-	√

which corresponds to the deprotonated esculetin ion. In the MS/MS analysis, we found a successive CO loss corresponding to the $[M-H-CO]^-$ *m/z* 149 and $[M-H-2CO]^-$ *m/z* 121 fragment ions [20].

The compounds of 3,4-dicaffeoylquinic acid, 3,5-dicaffeoylquinic acid, and 4,5-dicaffeoylquinic acid are identified by a signal at *m/z* 515 $[M-H]^-$. The MS^2 base peak is at *m/z* 353, indicating the loss of one of the caffeoyl [M-H-caffeoyl] groups for all three compounds. These three compounds are identified by the presence of signals at *m/z* 515 [M-H]. The caffeoylquinic acid ion is fragmented further to form *m/z* 354 [M-H-caffeoyl], 191 $[M-H-2C_9H_6O_3]^-$, 173 $[M-H-2C_9H_6O_3-H_2O]^-$, 135 $[M-C_7H_{10}O_5-C_9H_6O_3-COOH]^-$, and 179 $[M-H-C_9H_6O_3-$

$C_7H_{10}O_5]^-$ [21-22]. The MS^2 base peak for 3,4-dicaffeoylquinic acid is at *m/z* 354, while 3,5-dicaffeoylquinic and 4,5-dicaffeoylquinic acids are at *m/z* 191 and 173 base peaks, respectively. Three compounds have been reported to be used as anti-influenza viral, antioxidant, anti-apoptotic, anti-inflammatory, and anti-pigmentation activities [23-24].

Flavonoids

In this study, ten compounds are identified that belong to the flavonoids. One of the compounds is luteolin 7-rutinoside with *m/z* 593 $[M-H]^-$ and fragmentation at *m/z* 285, marking the disaccharide loss of rutinoside [25]. The loss of 308 Da is also found in kaempferol-3-*O*-rutinoside. Astragalin (kaempferol 3-*O*-glucoside) is one of the characteristic compounds found in *G. procumbens*. This compound produces MS1 ions at *m/z* 447 $[M-H]^-$ and a secondary MS^2 ion at *m/z* 285, 255, and 227 represent the typical MS/MS pattern of the kaempferol derivative in negative ion mode (Fig. 3) [26-27]. Astragalin has been reported as anti-inflammatory, antioxidant, neuroprotective, cardioprotective, antiobesity, antiosteoporotic, anticancer, antiulcer, and antidiabetic [28].

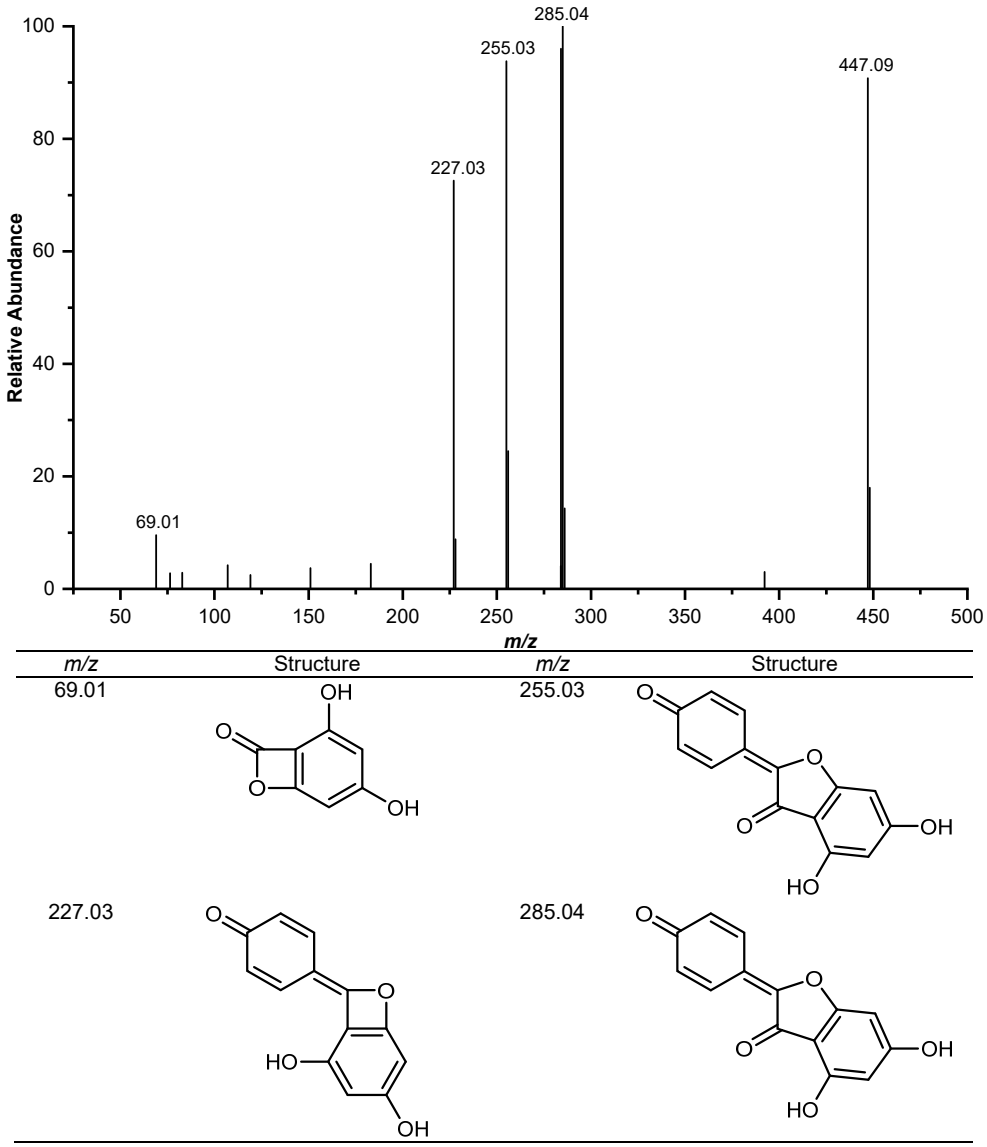

Fig 3. ESI-MS/MS ion negative spectra of astragalin

Fatty Acids

The quercetin-3-*O*-glucoside compound produces deprotonated ions at *m/z* 463. The MS fragment of this compound appears at *m/z* 301, which shows a loss of hexose unit (162 Da). Moreover, *m/z* 301 indicates the presence of quercetin [29]. The compound baicalin, which has antiviral, anti-inflammatory, antioxidant, and anti-apoptotic activity [30], exhibits $[M-H]^-$ at 445 and the aglycone anion at 269 (also with partial loss of glucuronic acid). In the MS^2 spectrum, a fragment at 269 yields three anions at 251, 241, and 223. These fragments may be due to the loss of H_2O, CO, and H_2O and CO, respectively [31].

Other Groups

Another compound identified is 4-(2-hydroxypropoxy)-3,5-dimethyl-phenol, detected at *m/z* 197 $[M+H]^+$. The compounds (-)-12-hydroxy-9,10-dihydrojasmonic acid (oxomonocarboxylic acid group) and harderoporphyrin (porphyrin group) are detected in negative ionization mode, with *m/z* being *m/z* 227 and *m/z* 609, respectively. These compounds are chlorophyll breakdown (Pa) products such as pheophorbide A with a monoisotopic mass of 592.26553 and produce fragmentation at *m/z* 593, 565, 533, 505, and 460 [31].

Clustering of Compounds in the Extracts

The PCA score plot (Fig. 4) shows that the leave and stem extracts were clustered according to their respective groups using the 31 detected compound band area as the variable. The score plot obtained could explain 96% of the total variation (PC1 = 92% and PC2 = 4%). These two parts of plants can be grouped well based on PC1. The detected compounds in the leaves sample tend to be clustered in PC1 negative values, and the stem is clustered in PC1 positive values. However, the distance between the two groups is close, indicating that the two groups are similar in composition and concentration of the compounds identified in the leaves and stems.

Variables that affect the clustering results can be observed in the PCA biplot, which combines the score and loading plots (Fig. 5). The PCA biplot shows objects and variables on a low-dimensional graph simultaneously so that the variables can be visually analyzed. The compound that significantly contributes to the differences between groups is the variable farthest from the main group (PC). In the PCA biplot, pheophorbide A and citric acid lead to a negative value of PC1, and the position was close to leaves clustering, so it can be concluded that these two compounds affect

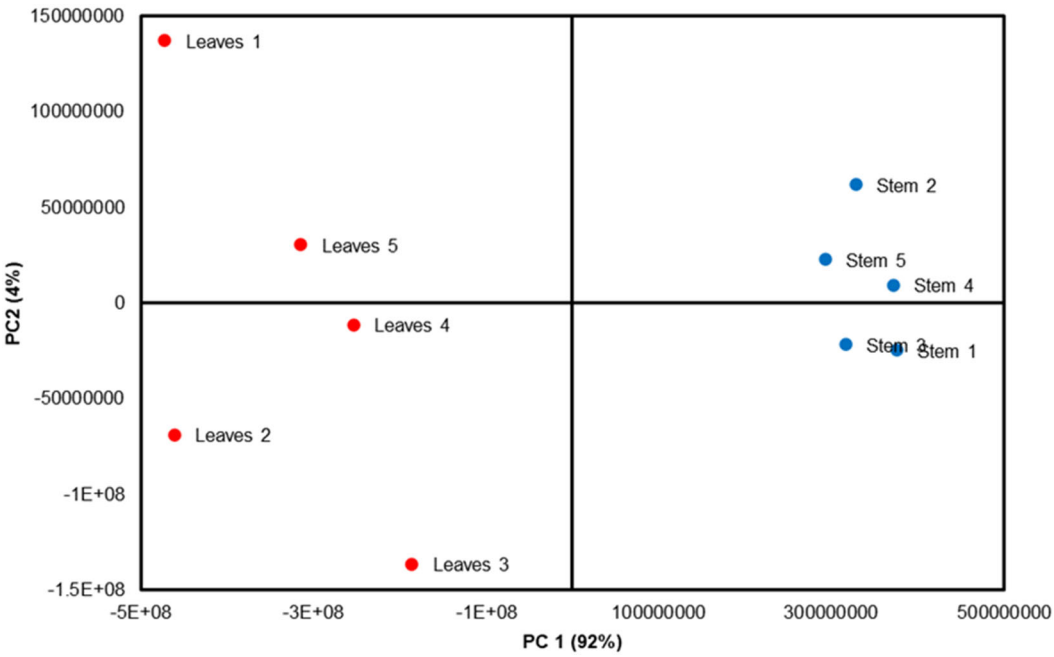

Fig 4. PCA score plot of metabolites in *G. procumbens* stem (●) and leaves (●) extracts

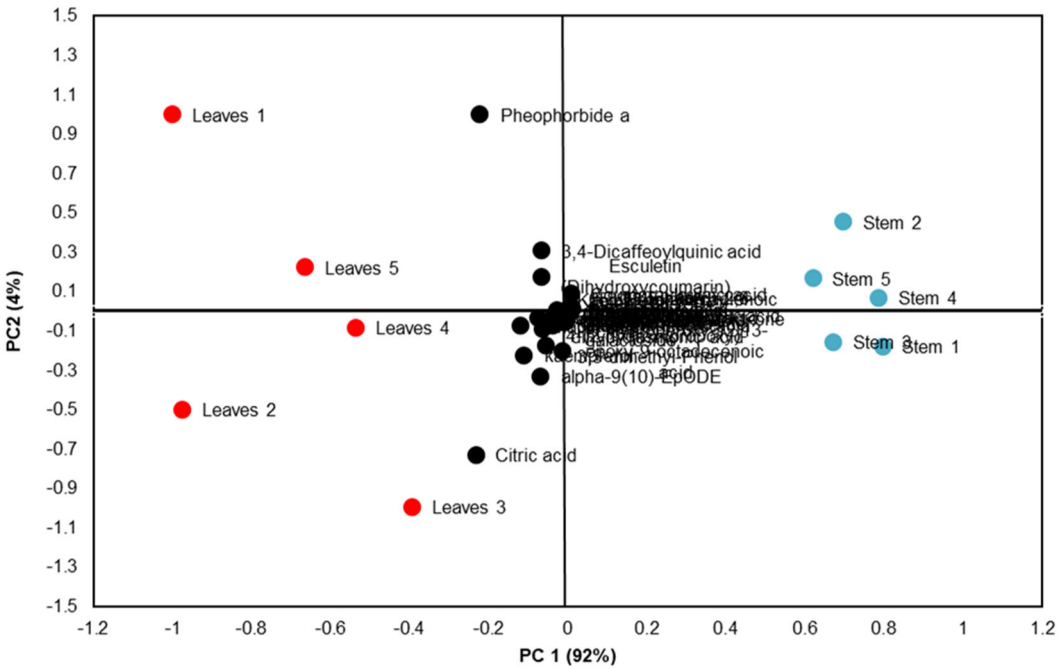

Fig 5. PCA biplot of metabolites extracted from *G. procumbens*

the grouping of leaves. On the other hand, according to the enlargement biplot, the stem was influenced by hesperetin and 5,8,12-trihydroxy-9-octadecenoic acid.

CONCLUSION

In this work, UHPLC-Q-Orbitrap HRMS analysis has been used to identify the metabolite profiles from the leaves and the stem of *G. procumbens*. There are 31 putative identified metabolites present in *G. procumbens*, such as members of phenolic acids, flavonoids, phenols, fatty acids, oxo monocarboxylic acids, porphyrins, and chlorophyll breakdown products. The clustering of the plant parts extract was achieved using the identified metabolite peak areas using PCA. The grouping is influenced by the presence of pheophorbide A and citric acid compounds.

ACKNOWLEDGMENTS

The authors gratefully acknowledged the Ministry of Research, Technology, and Higher Education of the Republic of Indonesia through *Penelitian Unggulan Dasar Perguruan Tinggi* Research Grant for this research (No: 4020/IT3.L1/PN/2020). A preprint (abstract) has previously been presented and published at the 9th International Conference of the Indonesian Chemical Society (ICICS) 2021, Mataram, Indonesia, 11-13 August 2021.

AUTHOR CONTRIBUTIONS

D.A.S. did the investigation, formal analysis, methodology, and write the original draft. C.A.P. did the formal analysis and visualization. I.H.S. and S.S.A. did the conceptualization, methodology, supervision, review, and editing. R.H. did the conceptualization, methodology, and validation. M.R. did the conceptualization, methodology, investigation, funding acquisition, supervision, review, and editing. All authors agreed to the final version of this manuscript.

REFERENCES

[1] Akhi, T.M.N., Adib, M., Islam, Q.S., Sultana, I., Haider, R., and Ibrahim, M., 2019, Preliminary phytochemical screening and assessment of pharmacological activities of leaves and stems of *Gynura procumbens* (Lour.) Merr, *Bangladesh Pharm. J.*, 22 (1), 79–84.

[2] Ashraf, K., Halim, H., Lim, M.S., Ramasamy, K., and Sultan, S., 2020, *In vitro* antioxidant, antimicrobial and antiproliferative studies of four different extracts of *Orthosiphon stamineus*, *Gynura*

procumbens and *Ficus deltoidea*, *Saudi J. Biol. Sci.*, 27 (1), 417–432.

[3] Tristantini, D., Setiawan, H., and Santoso, L.L., 2021, Feasibility assessment of an encapsulated longevity spinach (*Gynura procumbens* L.) extract plant in Indonesia, *Appl. Sci.*, 11 (9), 4093.

[4] Manogaran, M., Lim, V., and Mohamed, R., 2019, Phytoconstituents of the *Gynura procumbens* ethanol leaf extract and its fractions and their effects on viability of macrophages, *J. HerbMed Pharmacol.*, 8 (3), 224–230.

[5] Chandradevan, M., Simoh, S., Mediani, A., Ismail, N.H., Ismail, I.S., and Abas, F, 2020, UHPLC-ESI-Orbitrap-MS analysis of biologically active extracts from *Gynura procumbens* (Lour.) Merr. and *Cleome gynandra* L. leaves, *Evidence-Based Complementary Altern. Med.*, 2020, 3238561.

[6] Siregar, D.R., and Silitonga, P.M., 2021, The effect of sambung nyawa leaf extract (*Gynura Procumbens*) on albumin and globulin of rats (*Rattus novergicus*) serum induced by *E. coli* bacteria, *IJCST*, 4 (1), 29–33.

[7] Zoyane, S., Chen, L., Xu, M.J., Gong, Z.N., Xu, S., and Makunga, N.P., 2019, Geographic-based metabolomic variation and toxicity analysis of *Sutherlandia frutescens* L. R.Br. – An emerging medicinal crop in South Africa, *Ind. Crops Prod.*, 133, 414–423.

[8] Rafi, M., Handayani, F., Darusman, L.K., Rohaeti, E., Wahyu, Y., Sulistiyani, S., Honda, K., and Putri, S.P., 2018, A combination of simultaneous quantification of four triterpenes and fingerprint analysis using HPLC for rapid identification of *Centella asiatica* from its related plants and classification based on cultivation ages, *Ind. Crops Prod.*, 122, 93–97.

[9] Ng, Z.X., Yong, P.H., and Lim, S.Y., 2020, Customized drying treatments increased the extraction of phytochemicals and antioxidant activity from economically viable medicinal plants, *Ind. Crops Prod.*, 155, 112815.

[10] Llorent-Martínez, E.J., Zengin, G., Sinan, K.I., Polat, R., Canlı, D., Picot-Allain, M.C.N., and Mahomoodally, M.F., 2020, Impact of different extraction solvents and techniques on the biological activities of *Cirsiumy ildizianum* (Asteraceae: Cynareae), *Ind. Crops Prod.*, 144, 112033.

[11] Guo, N., Yang, D., Liu, C., Yan, H., Yang, X., Wang, X., and Fan, B., 2020, Metabolite profiling of Huaiyang *Medicago polymorpha* with different mowing crops, *Nat. Prod. Res.*, 34 (15), 2238–2242.

[12] Septaningsih, D.A., Putra, C.A., Suparto, I.H., Achmadi, S.S., Heryanto, R., and Rafi, M., 2021, *Phytochemical profiling of* Gynura procumbens *leaves and stem extracts using UHPLC-Q-Orbitrap HRMS*, https://icics2021.unram.ac.id/ics/abstracts?page=6, accessed on 29th November 2021.

[13] Ningsih, R., Rafi, M., Tjahjoleksono, A., Bintang, M., and Megia, R., 2021, Ripe pulp metabolite profiling of ten Indonesian dessert banana cultivars using UHPLC-Q-Orbitrap HRMS, *Eur. Food Res. Technol.*, 247 (11), 2821–2830.

[14] Cai, R., Li, Y., Clément, Y., Li, D., Dubois, C., Fabre, M., Besson, L., Perrier, S., George, C., Ehn, M., Huang, C., Yi, P., Ma, Y., and Riva, M., 2021, Orbitool: A software tool for analyzing online orbitrap mass spectrometry data, *Atmos. Meas. Tech.*, 14 (3), 2377–2387.

[15] Cook-Botelho, J.C., Bachmann, L.M., and French, D., 2017, "Chapter 10 - Steroid Hormones" in *Mass Spectrometry for the Clinical Laboratory*, Eds. Nair, H., and Clarke, W., Academic Press, San Diego, US, 205-230.

[16] Kumar, B.R., 2017., Application of HPLC and ESI-MS techniques in the analysis of phenolic acids and flavonoids from green leafy vegetables (GLVs), *J. Pharm. Anal.*, 7 (6), 349–364.

[17] Nićiforović, N., and Abramovič, H., 2013, Sinapic acid and its derivatives: Natural sources and bioactivity, *Compr. Rev. Food Sci. Food Saf.*, 13 (1), 34–51.

[18] Pei, K., Ou, J., Huang, J., and Ou, S., 2015, *p*-Coumaric acid and its conjugates: Dietary sources, pharmacokinetic properties and biological activities, *J. Sci. Food Agric.*, 96 (9), 2952–2962.

[19] Espíndola, K., Ferreira, R.G., Narvaez, L., Silva Rosario, A., da Silva, A., Silva, A., Vieira, A., and Monteiro, C.M., 2019, Chemical and

pharmacological aspects of caffeic acid and its activity in hepatocarcinoma, *Front. Oncol.*, 9, 541.

[20] Kim, J.S., Ha, T.Y., Ahn, J., and Kim, S., 2014, Analysis and distribution of esculetin in plasma and tissues of rats after oral administration, *Prev. Nutr. Food Sci.*, 19 (4), 321–336.

[21] Wan, C., Yu, Y., Zhou, S., Tian, S., and Cao, S., 2011, Isolation and identification of phenolic compounds from *Gynura divaricata* leaves, *Pharmacogn. Mag.*, 7 (26), 101–108.

[22] Chen, F., Long, X., Liu, Z., Shao, H., and Liu, L., 2014, Analysis of phenolic acids of Jerusalem artichoke (*Helianthus tuberosus* L.) responding to salt-stress by liquid chromatography/tandem mass spectrometry, *Sci. World J.*, 2014, 568043.

[23] El Baaboua, A., El Maadoudi, M., Bouyahya, A., Belmehdi, O., Kounnoun, A., Zahli, R., and Abrini, J., 2018, Evaluation of antimicrobial activity of four organic acids used in chicks feed to control *Salmonella typhimurium*: Suggestion of amendment in the search standard, *Int. J. Microbiol.*, 2018, 7352593.

[24] Tabassum, N., Lee, J.H., Yim, S.H., Batkhuu, G.J., Jung, D.W., and Williams, D.R., 2016, Isolation of 4,5-*O*-dicaffeoylquinic acid as a pigmentation inhibitor occurring in *Artemisia capillaris* Thunberg and its validation *in vivo*, *Evidence-Based Complementary Altern. Med.*, 2016, 7823541.

[25] Plazonić, A., Bucar, F., Maleŝ, Ž., Mornar, A., Nigović, B., and Kujundžić, N., 2009, Identification and quantification of flavonoids and phenolic acids in burr parsley (*Caucalis platycarpos* L.), using high-performance liquid chromatography with diode array detection and electrospray ionization mass spectrometry, *Molecules*, 14 (7), 2466–2490.

[26] Fu, B., Ji, X., Zhao, M., He, F., Wang, X., Wang, Y., Liu, P., and Niu, L., 2016, The influence of light quality on the accumulation of flavonoids in tobacco (*Nicotiana tabacum* L.) leaves, *J. Photochem. Photobiol., B*, 162, 544–549.

[27] Xiaofeng, Y., Shuang, Z., Li, Z., Dan, W., Xiaoman, F., and Zhen, O., 2019, Effect of frost on flavonol glycosides accumulation and antioxidant activities of mulberry (*Morus alba* L.) leaves, *Pharmacogn. Mag.*, 15 (63), 466–472.

[28] Riaz, A., Rasul, A., Hussain, G., Zahoor, M.K., Jabeen, F., Subhani, Z., Younis, T., Ali, M., Sarfraz, I., and Selamoglu, Z., 2018, Astragalin: A bioactive phytochemical with potential therapeutic activities, *Adv. Pharmacol. Pharm. Sci.*, 2018, 9794625.

[29] Li, Z.H., Guo, H., Xu, W.B., Ge, J., Li, X., Alimu, M., and He, D.J., 2016, Rapid identification of flavonoid constituents directly from PTP1B inhibitive extract of raspberry (*Rubus idaeus* L.) leaves by HPLC–ESI–QTOF–MS-MS, *J. Chromatogr. Sci.*, 54 (5), 805–810.

[30] Gupta, A., and Pandey, A.K., 2019, "Plant Secondary Metabolites with Hepatoprotective Efficacy" in *Nutraceuticals and Natural Product Pharmaceuticals*, Eds. Galanakis, C.M., Academic Press, Cambridge, US, 71–104.

[31] Li, K., Fan, H., Yin, P., Yang, L., Xue, Q., Li, X., Sun, L., and Liu, Y., 2018, Structure-activity relationship of eight high content flavonoids analyzed with a preliminary assign-score method and their contribution to antioxidant ability of flavonoids-rich extract from *Scutellaria baicalensis* shoots, *Arabian J. Chem.*, 11 (2), 159–170.